Online (ex-N1BWT)
W1GHZ Microwave Antenna Book

Chapter 6
Feeds for Parabolic Dish Antennas
Paul Wade W1GHZ ©1998,1999

Section 6.5 Dual-Mode Feedhorns

6.5.3 Diagonal Horn

The diagonal horn antenna was probably the first successful multi-mode feed horn. A square horn excited with only the dominant $\mathbf{TE_{01}}$ waveguide mode has a radiation pattern which is not symmetrical, as we saw in Figure 6.4-10. The asymmetry is caused by E-plane edge currents in the walls of horn, the same problem found in conical horns. A. W. Love[11] found that exciting an additional mode, the $\mathbf{TE_{10}}$ mode, orthogonal to the original $\mathbf{TE_{01}}$ mode, results in radiation which is polarized along the diagonals of the horn. The resulting symmetry produces a radiation pattern with symmetrical E- and H-planes, suitable for linear or circular polarization. The field at the diagonal horn aperture is similar to the field in a circular horn feed, illustrated in Figure 6.5-20.

The diagonal horn may be designed for a wide range of ***f*/D** by varying the square dimension of the horn aperture. Love gives approximate beamwidths of **58.5 λ/d** for 3 dB beamwidth and **101 λ/d** for 10 dB beamwidth, where **d** is the dimension of one side of the square aperture. Patterns are best with small flare angles, less than 30°. The diagonal horn does have sidelobes in the 45° pattern cuts (planes at angles halfway between the E- and H-planes), and these sidelobes have larger amplitudes as the flare angle increases.

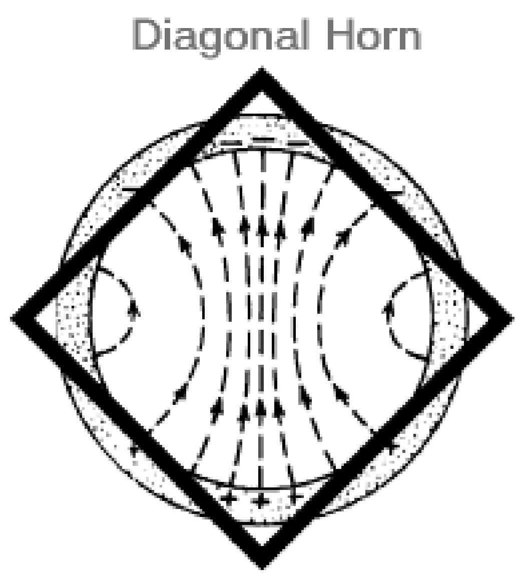

Figure 6.5-20

Love generates the additional mode to produce the diagonal pattern in a circular transition from rectangular waveguide to the square horn. However, N7ART[12] excites diagonal horns for 1296 MHz with a diagonal dipole inside the square waveguide, as shown in Figure 6.5-21. W2IMU shows the same technique in the *ARRL UHF/Microwave Experimenters Manual*[13]. Circular polarization may be produced by two crossed dipoles with 90° phase shift.

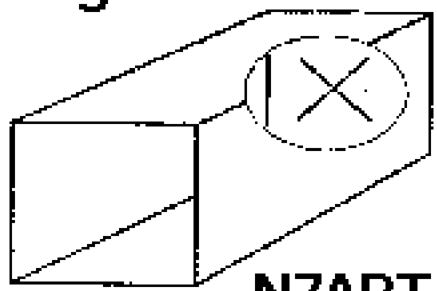

The N7ART article describes a series of horns for ***f*/D** from about 0.3 to 0.4. Most of these horns are simple open-ended square waveguides with no flare. The smallest, with each square side 129.5 mm long, or 0.603λ at 1296 MHz — any smaller would probably be beyond waveguide cutoff. The radiation pattern calculated by **NEC2** in Figure 6.5-22 shows good efficiency for ***f*/D** around 0.3, with the phase center at the center of the aperture. The calculated pattern is quite symmetrical, including the 45 degree planes as well as the E- and H-planes. Efficiency is reduced by a poor front-to-back ratio, just as we saw for open-ended rectangular and circular waveguide feeds.

The pattern calculated by **NEC2** in Figure 6.5-23, for a slightly larger version, 139.7 mm square, shows slightly better efficiency for ***f*/D** around 0.32. A larger size, 146.1 mm square shown in Figure 6.5-24, has best efficiency around ***f*/D**=0.35, while the largest plain diagonal waveguide version, 157.5 mm square, has best efficiency for ***f*/D** around 0.37, as shown in Figure 6.5-25. All these unflared diagonal horns have good pattern symmetry with the phase center at the center of the aperture. As the size of the unflared diagonal horn increases, the calculated **NEC2** patterns show improving front-to-back ratio resulting in improving efficiency.

N7ART also described a flared diagonal horn for 1296 MHz, flaring out from the square waveguide to a 7 inch (177 mm) square aperture. The flare is gradual, as recommended by Love, with a 10.2° full flare angle. The radiation pattern calculated using P.O. is shown in Figure 6.5-26, with best efficiency for ***f*/D** around 0.4, and a phase center just inside the center of the aperture. Calculated 45 degree patterns are almost identical to the E- and H-planes, so symmetry is excellent. The rear null in the pattern is an artifact of the Physical Optics calculations.

These calculated patterns are slightly broader at the –10 dB points than measured by N7ART, and the calculated ***f*/D** for best efficiencies are very close to the ***f*/D** he recommends for lowest noise (best **G/T**), but lower than the ***f*/D** he recommends for maximum gain. I have more faith in measured data than computer simulations, so go with N7ART's suggestions.

Unflared diagonal horns appear to offer the best performance in a small physical size; for a small dish, this would minimize feed blockage for better overall efficiency. The symmetrical pattern allows good performance with circular polarization. Thus, for a small dish with circular polarization, like a 12-foot TVRO dish for 1296 MHz, the diagonal horn is probably the best feed available.

N7ART 1296 MHz diagonal horn 129.5 mm square, by NEC2

Figure 6.5-22

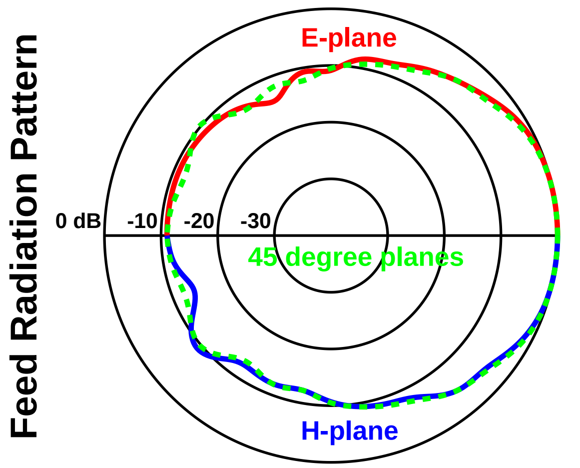

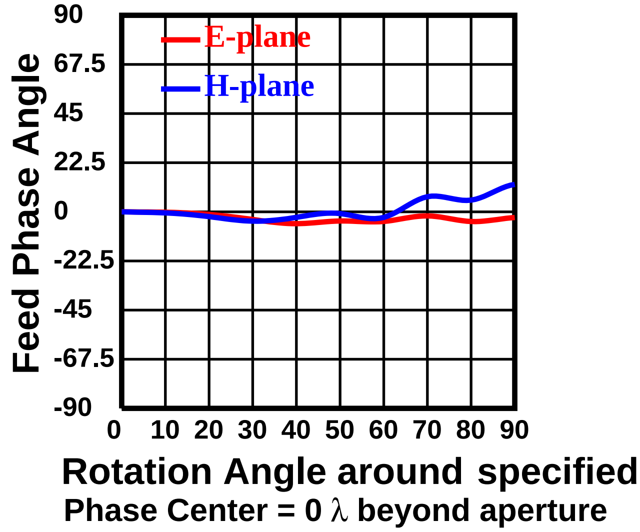

Dish diameter = 10 λ   Feed diameter = 1 λ

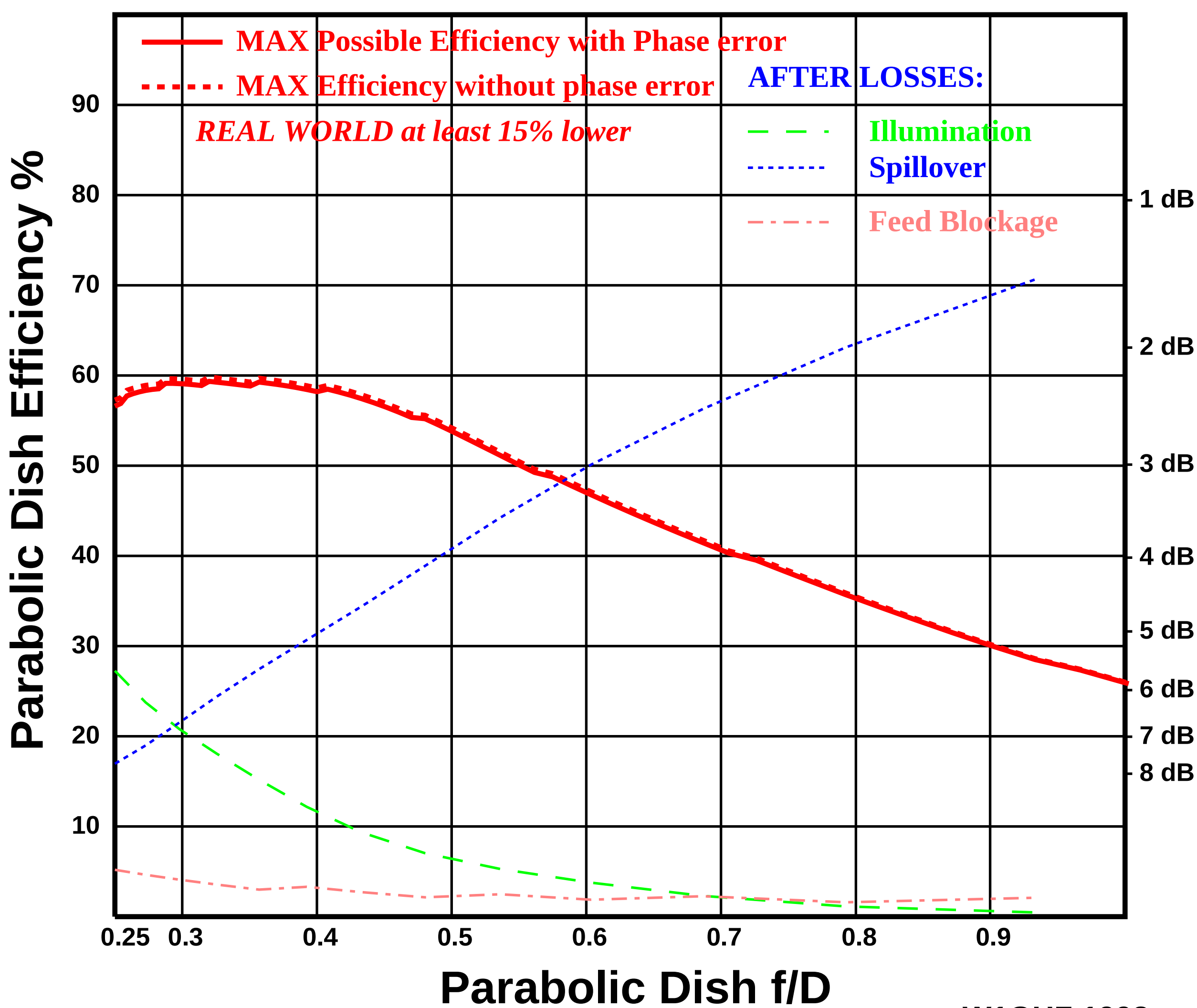

W1GHZ 1998

N7ART 1296 MHz diagonal horn, 139.7 mm square, by NEC2

Figure 6.5-23

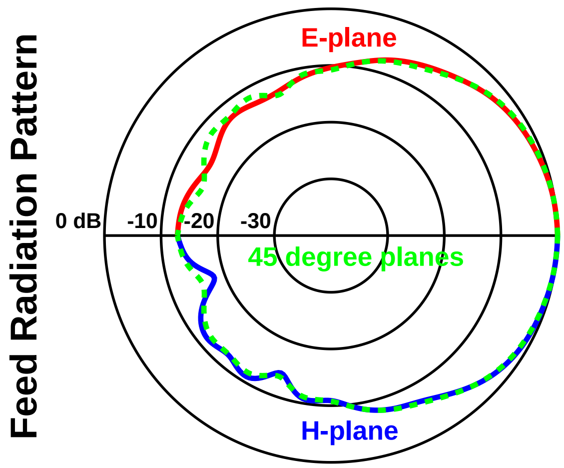

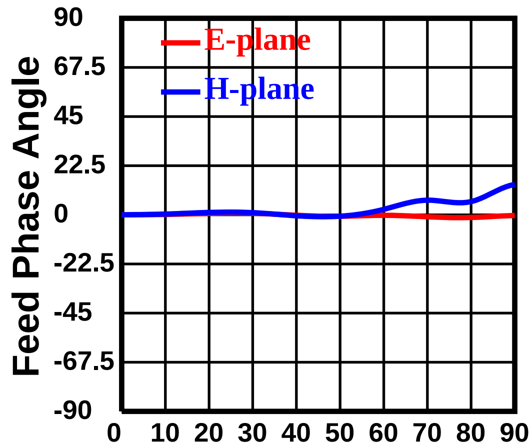

Dish diameter = 10 λ Feed diameter = 1 λ

Rotation Angle around specified Phase Center = 0 λ beyond aperture

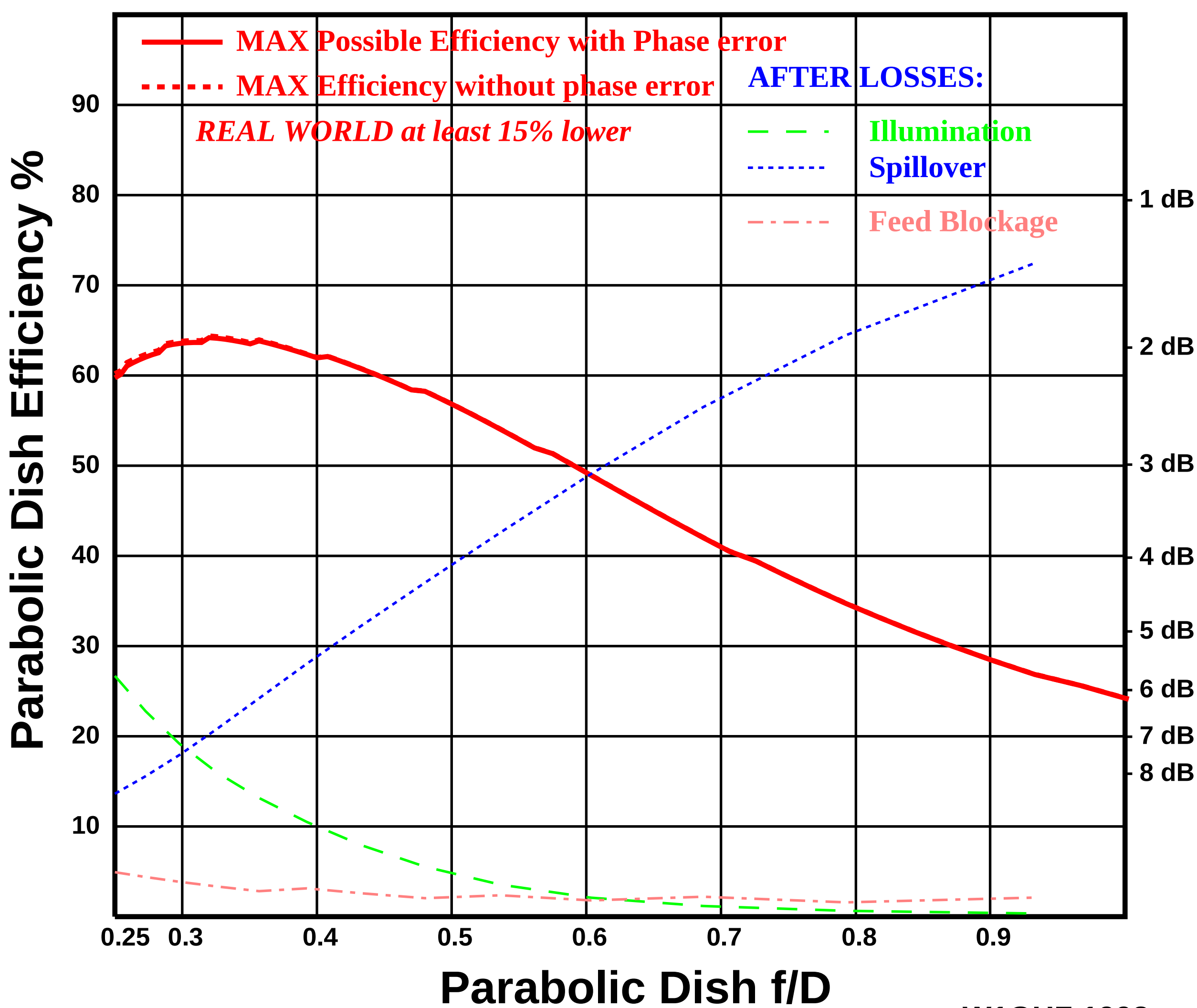

W1GHZ 1998

N7ART 1296 MHz diagonal horn 146.1 mm square, by NEC2

Figure 6.5-24

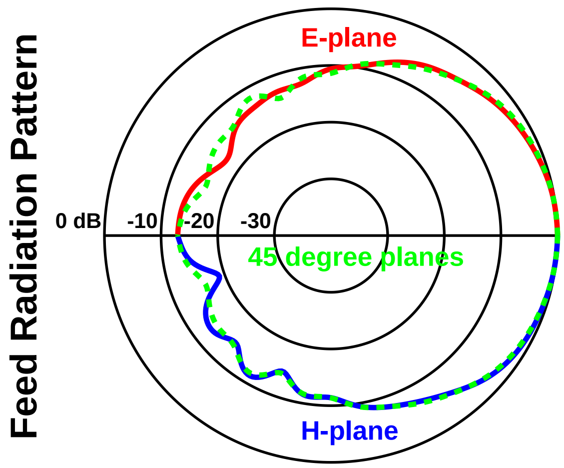

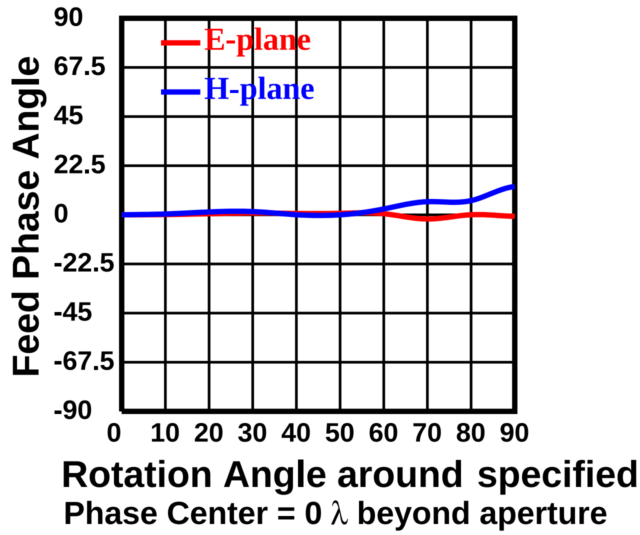

Dish diameter = 10 λ Feed diameter = 1 λ

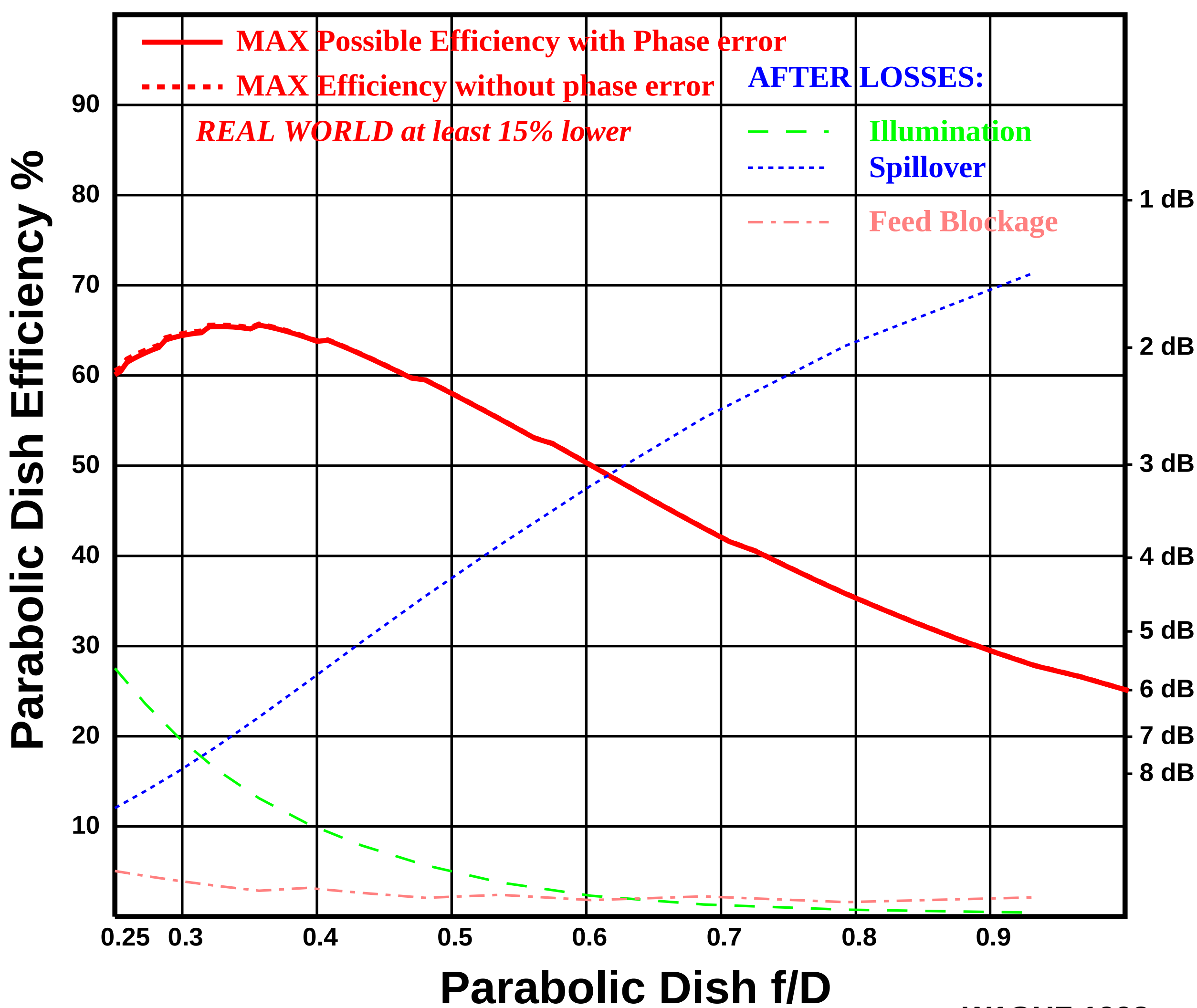

W1GHZ 1998

N7ART 1296 MHz diagonal horn 157.5 mm square, by NEC2

Figure 6.5-25

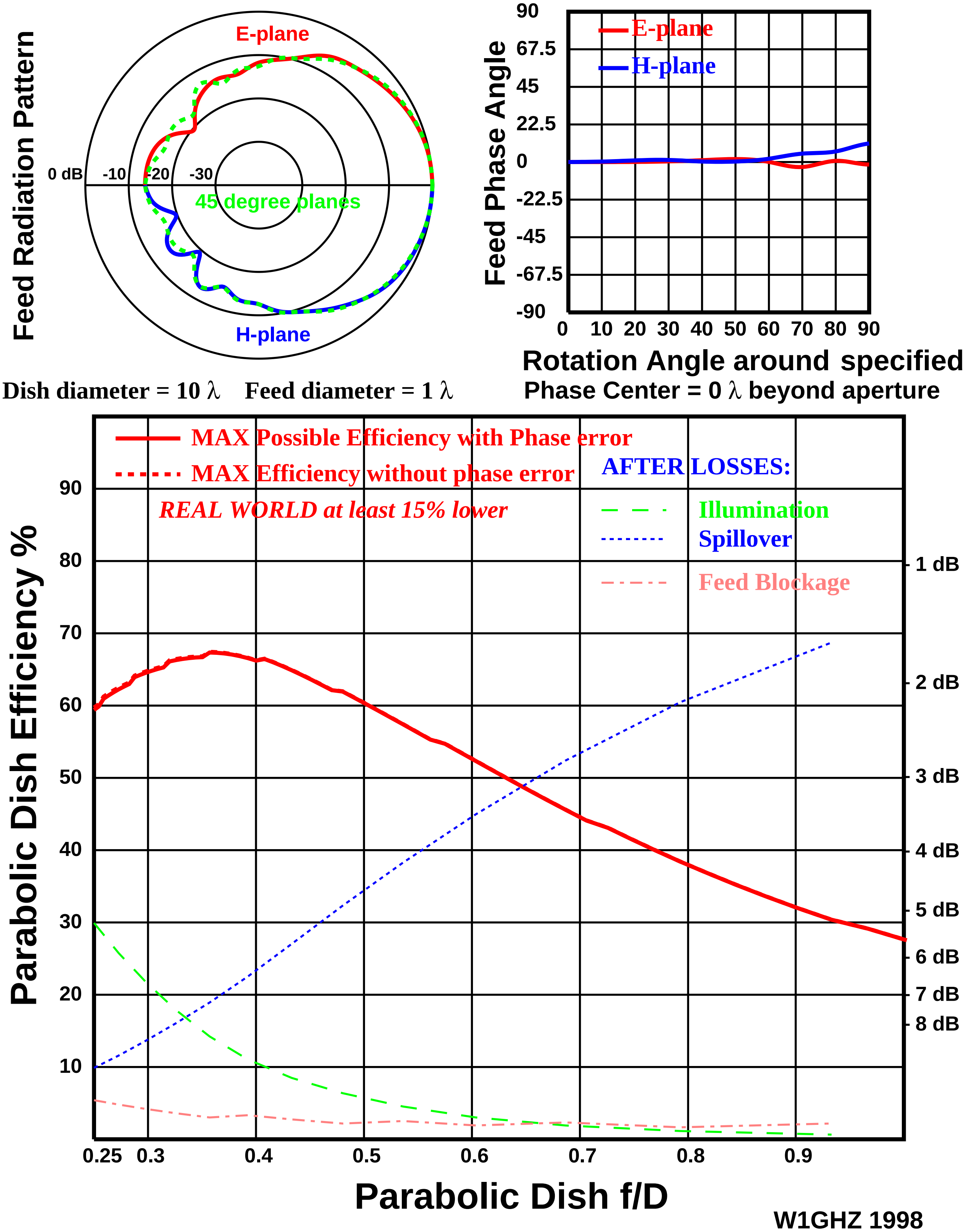

N7ART 1296 MHz diag horn, 7" square, 10.2 deg flare, by P.O.

Figure 6.5-26

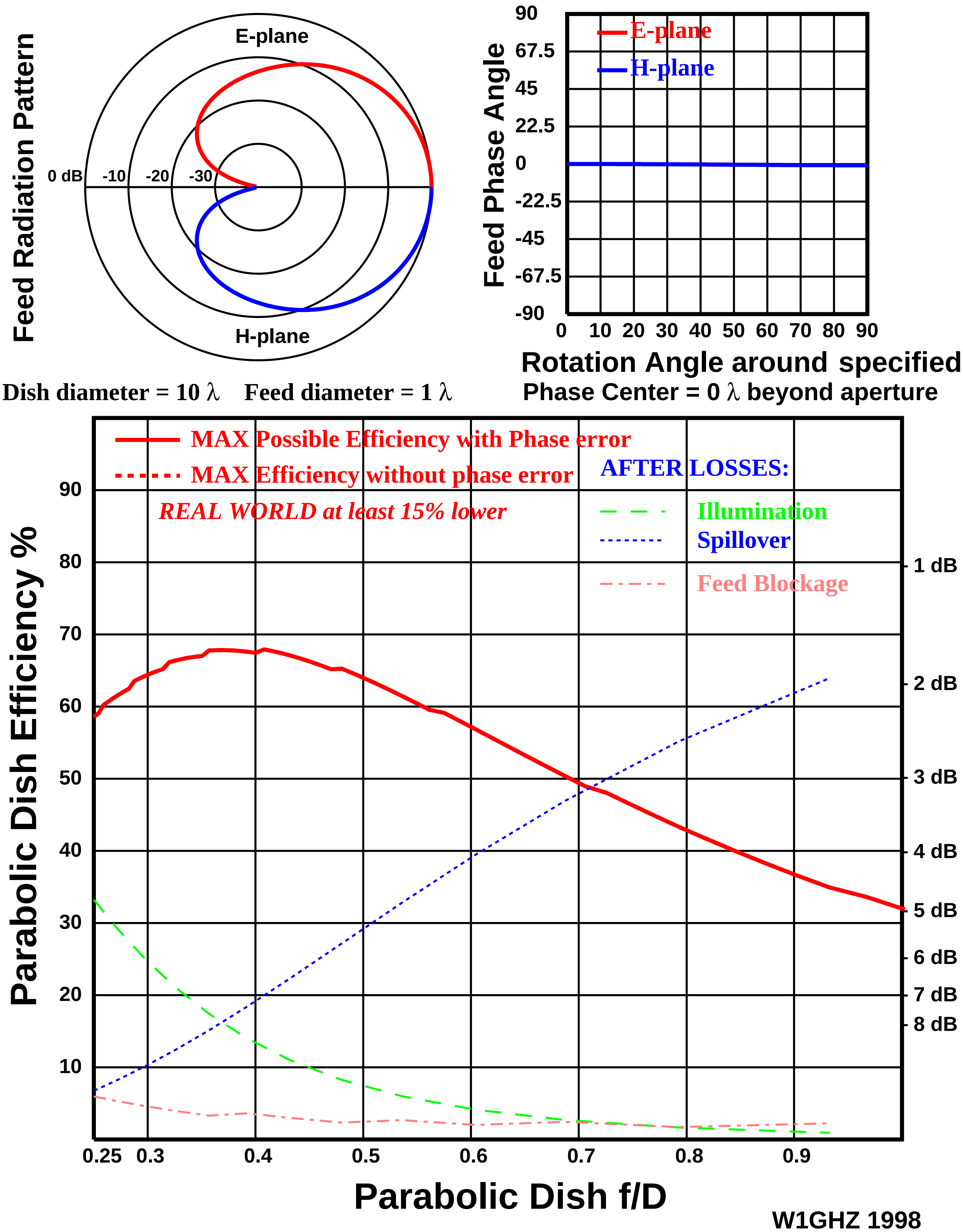

VE1ALQ takes advantage of the small size of the diagonal horn in a dual-band feed for 1296 and 432 MHz. In Figure 6.5-27, the diagonal horn for 1296 is in the center of a 432 MHz EIA dual-dipole feed. The phase center of the EIA feed, in Figure 6.2-6, is about 0.15λ behind the dipoles, while the diagonal horn phase center is at the center of the aperture. The photo shows that VE1ALQ has arrived at this combination empirically.

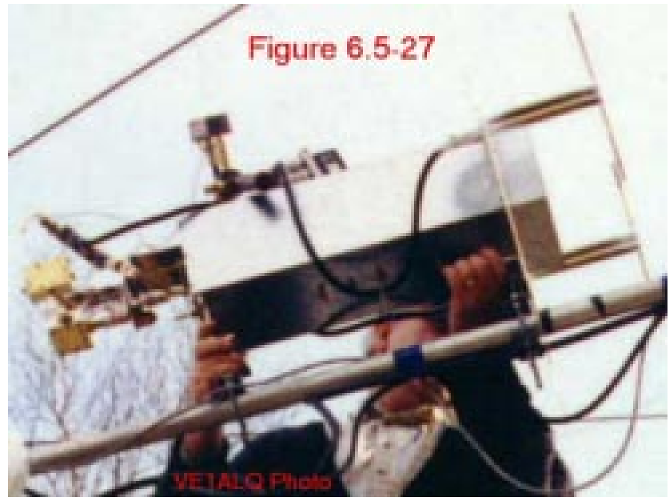

Diagonal horns can also be used for larger ***f*/D** by increasing the horn aperture size. For example, a DSS offset dish requires an illumination angle of about 75°, equivalent to an ***f*/D** of about 0.7. I used Love's estimate of **101 λ/d** for 10 dB beamwidth to estimate a desired aperture dimension of 1.35λ square. The calculated pattern with a 30° flare angle was a bit wide, so I increased the aperture dimension to 1.4λ square. Then I played with the flare angle. W2IMU[13] suggests a maximum of 7° half-angle, which would result in a rather long horn. Since Love[11] states that 45° sidelobes increase with flare angle, but doesn't say how much, I calculated patterns for 30° and 60° flare to compare with the 14° suggested by W2IMU.

The radiation pattern and efficiency calculated using P.O. for a 1.4λ square diagonal horn with 14° flare (full angle) are shown in Figure 6.5-28, with a clean pattern, small 45° sidelobes, and excellent efficiency for the offset dish equivalent ***f*/D** of about 0.7. The estimated phase center is about 0.07λ inside the aperture.

Increasing the flare angle to 30° resulted in slightly larger 45° sidelobes, as shown in Figure 6.5-29. Efficiency is very slightly lower than the longer horn, with the phase center 0.13λ inside the aperture. However, a 60° flare angle produces larger 45° sidelobes that lower the calculated efficiency noticeably, as shown in Figure 6.5-30. Phase center for this horn is 0.285λ inside the aperture.

Since the 30° flare angle provides excellent calculated efficiency, I decided to build this one, as well as the more compact 60° flare to see if the difference in performance would be measurable. I chose to excite these feed horns directly from

Template for
10.368 GHz Offset diagonal horn
1.4 wavelengths square
60 degree flare

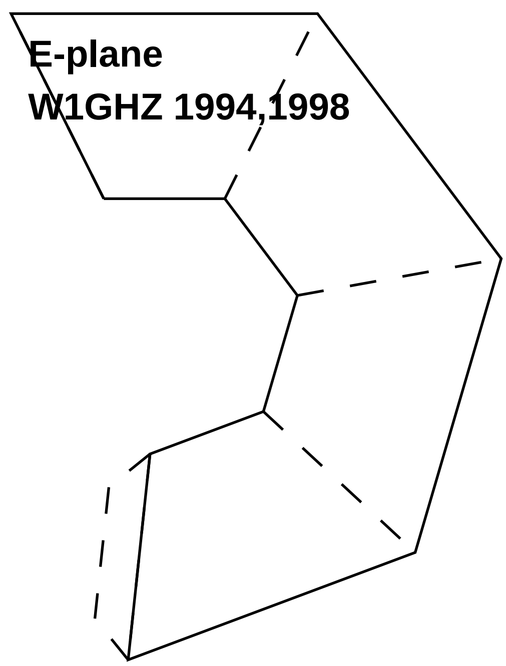

Figure 6.5-31

Offset diagonal horn, 1.4λ square, 14 degree full flare, by P.O.

Figure 6.5-28

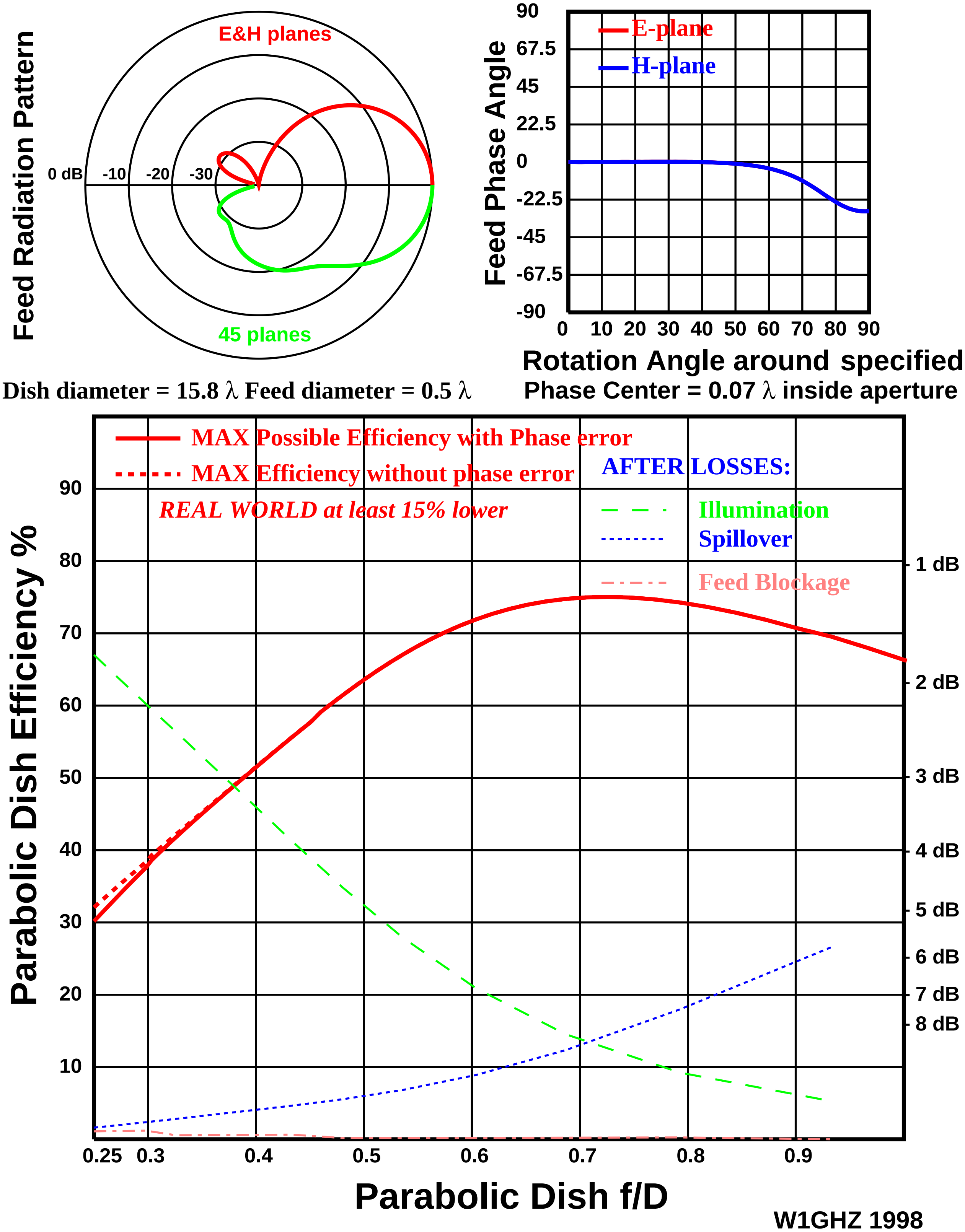

Offset diagonal horn 1.4λ square, 30 degree full flare, by P.O.

Figure 6.5-29

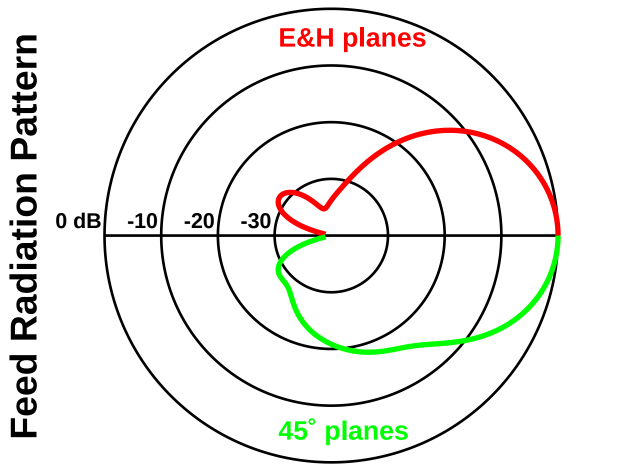

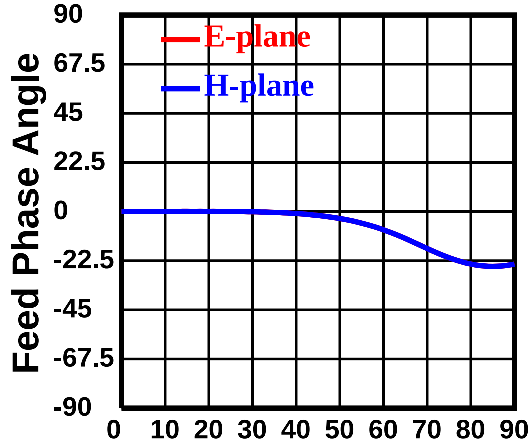

Rotation Angle around specified
Phase Center = 0.13 λ inside aperture

Dish diameter = 15.8 λ Feed diameter = 0.5 λ

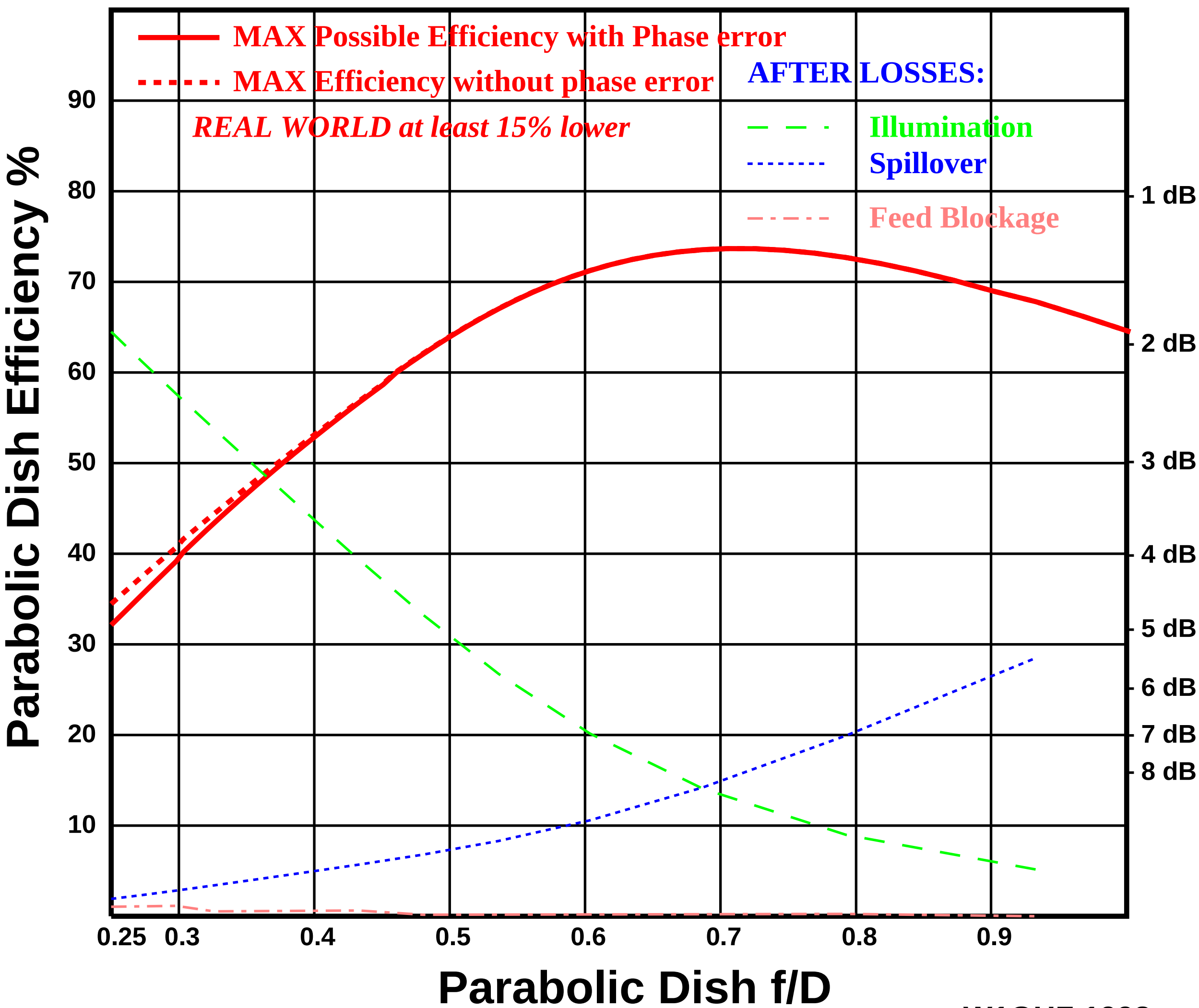

W1GHZ 1998

Offset diagonal horn, 1.4λ square, 60 degree full flare, by P.O.

Figure 6.5-30

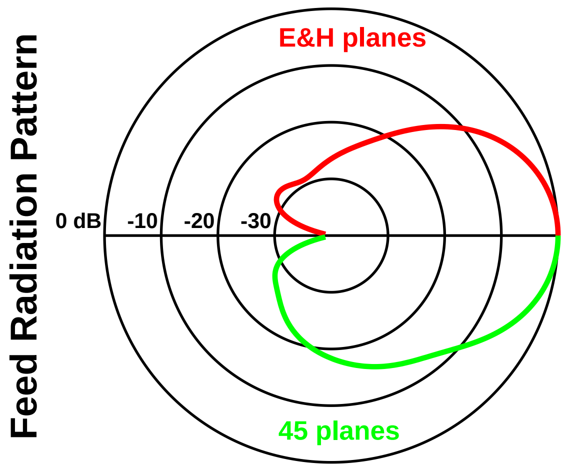

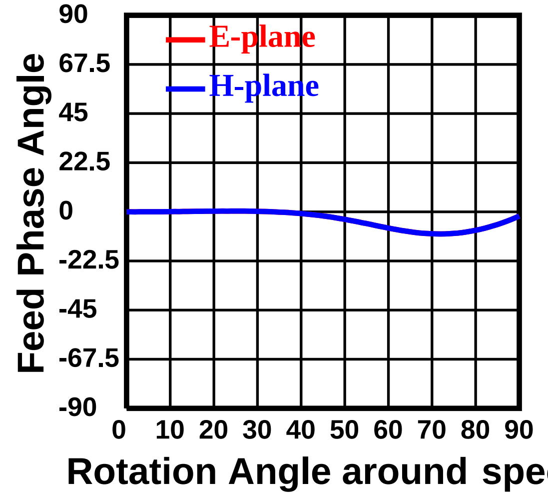

Dish diameter = 15.8 λ Feed diameter = 0.5 λ

Phase Center = 0.285 λ inside aperture

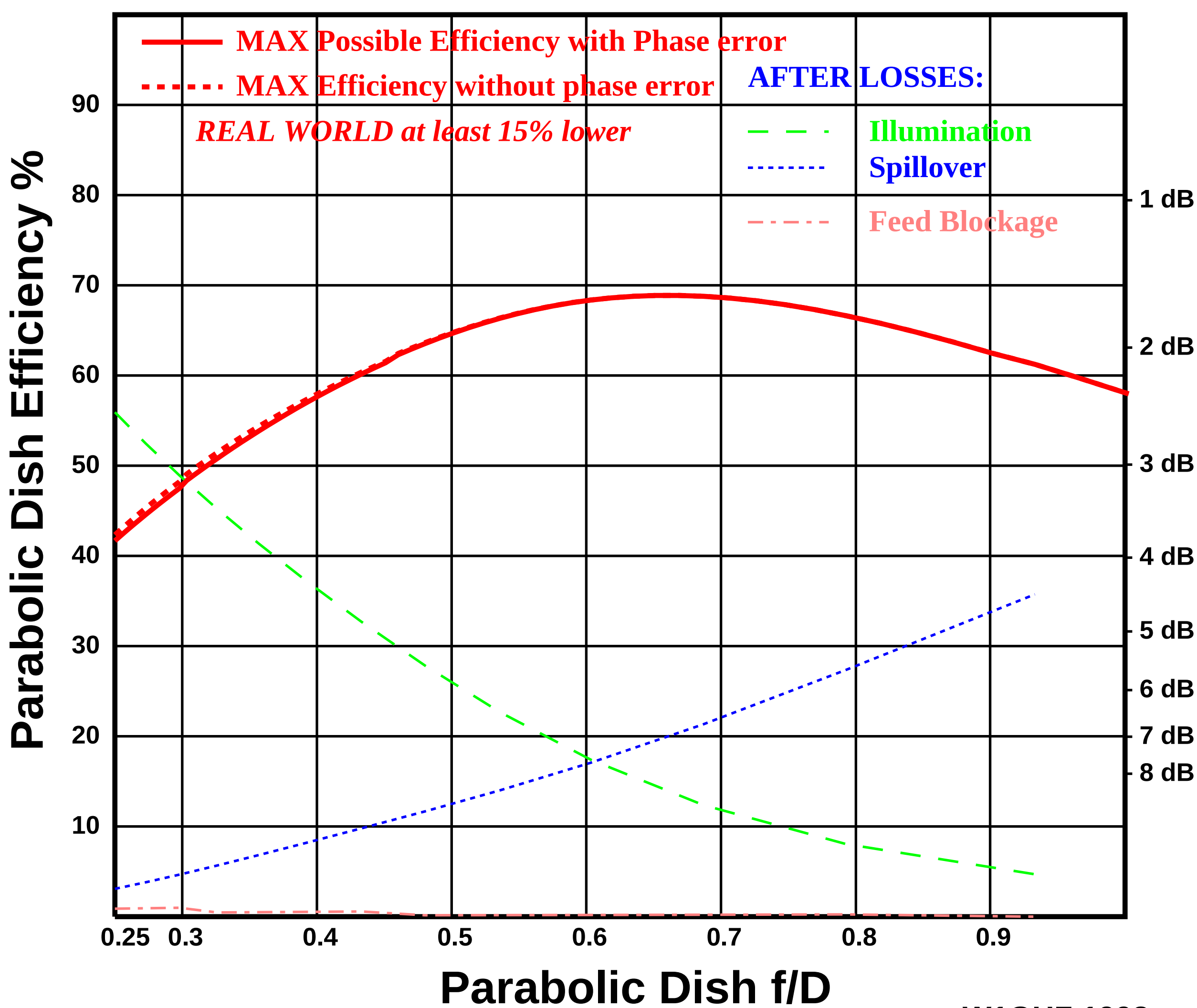

W1GHZ 1998

circular waveguide — at 10 GHz, the waveguide is ¾" copper water pipe. The transition to square cross-section was formed by hammering one end of the pipe on a square mandrel. Then the horn sections were cut from sheet copper using the **HDL_ANT** templates like Figure 6.5-31, and soldered to the square end of the waveguide transitions. The completed horns are shown in Figure 6.5-32.

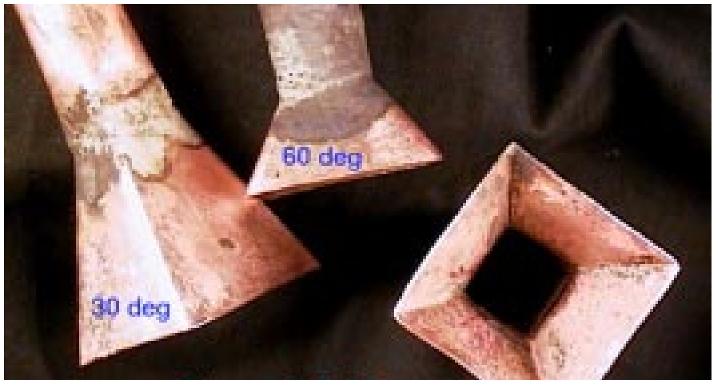

Figure 6.5-32

I made sun noise measurements on offset dishes fed with the diagonal horns in Figure 6.5-32 with disappointing results. The 30° flare horn yielded a measured efficiency of 45 to 47%, while the 60° flare version measured only 39% efficiency. I then rotated the polarization so that the horns would operate as square horns in the $\mathbf{TE}_{01}$ mode, like Figure 6.4-22. As square horns, the efficiency is several percent higher in both cases, while the calculated efficiencies were lower. My suspicion is that the short hammered transition from round to square cross-section does not properly launch the additional mode for diagonal horn operation; I will have to try ways to fabricate a better taper.

As an example of an even larger diagonal horn, I investigated one to feed a large Gregorian-style shaped reflector dish for Lyle, VK2ALU. This is intended as a 10 GHz replacement for the 12 GHz corrugated horn of Figure 6.4-22. The desired illumination angle for the subreflector is about 28°, but with a bit more than 10 dB edge taper. One possibility, the result of several trial calculations, is shown in Figure 6.5-33, with an aperture of 2.8λ and a flare angle of 30°. The pattern exhibits some significant sidelobes in the 45° planes; reducing the flare angle might improve these sidelobes, but would make the horn very long. The phase center for this large horn is 1.3 wavelengths inside the aperture. Because of the sidelobes, Lyle chose to investigate another alternative, described later in this section.

The diagonal horn has two attractive features as a feedhorn: its small size reduces blockage loss, and its square shape is relatively easy to fabricate. As we have seen from the examples, it is possible to dimension a diagonal horn for a full range of ***f*/D**. Disadvantages are the high sidelobe levels in the 45° planes, and the difficulty of interfacing to standard rectangular waveguide feedlines.

The sidelobe levels in the 45° planes are less of a disadvantage for ham use than in commercial applications. The 45° sidelobes tend to produce cross-polarized radiation, particularly with offset reflectors. Since most satellite broadcasting systems use polarization diversity to double the number of channels, cross-polarization is highly undesirable.

Diagonal horn, 2.8λ square, 30 degree flare, by P.O.

Figure 6.5-33

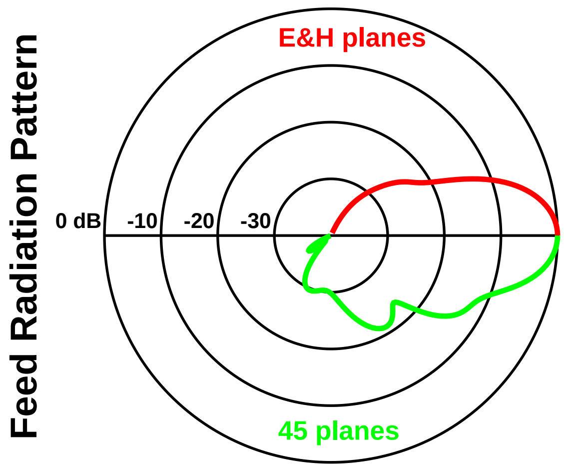

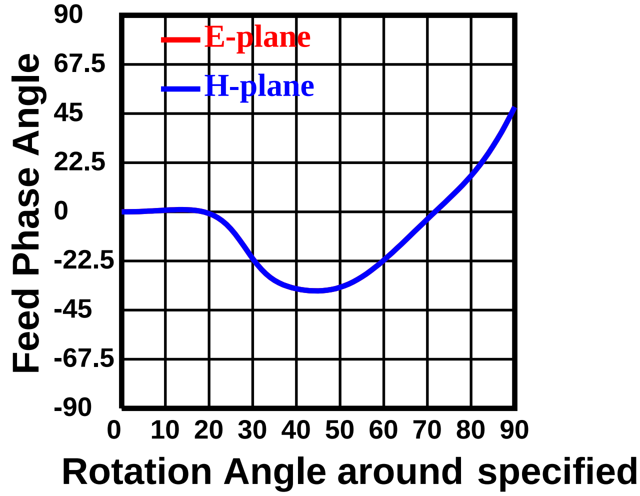

Dish diameter = 28 λ   Feed diameter = 2.8 λ

Phase Center = 1.3 λ inside aperture

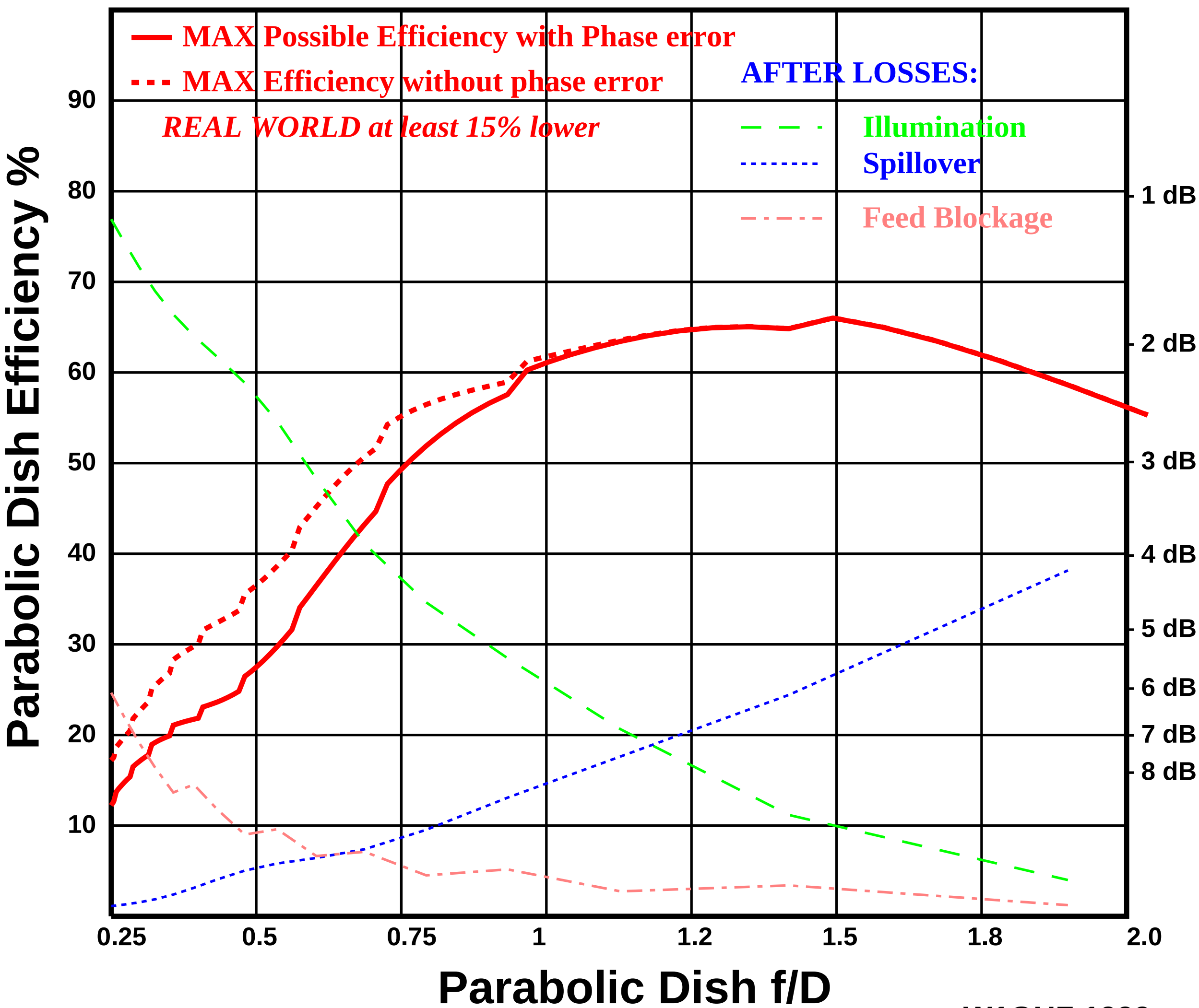

W1GHZ 1999

6.5.4 Potter dual-mode conical horn

After the diagonal horn, the next development in multi-mode feedhorns was the dual-mode conical horn by Potter[14]. This horn has better sidelobe levels than the diagonal horn, particularly in the 45° planes. It takes advantage of the symmetry of a conical horn while reducing the E-plane sidelobes we saw in section 6.4-1 by exciting the **TM**$_{11}$ mode in addition to the dominant **TE**$_{11}$ mode, with relative amplitudes so that the sidelobes produced by the two modes are out of phase and cancel, just as we saw in Figures 6.5-5 and 6.5-6. The Potter horn was apparently the inspiration for W2IMU to develop his dual-mode horn[1] discussed in section 6.5-1.

Potter dual-mode conical horn

Figure 6.5-34

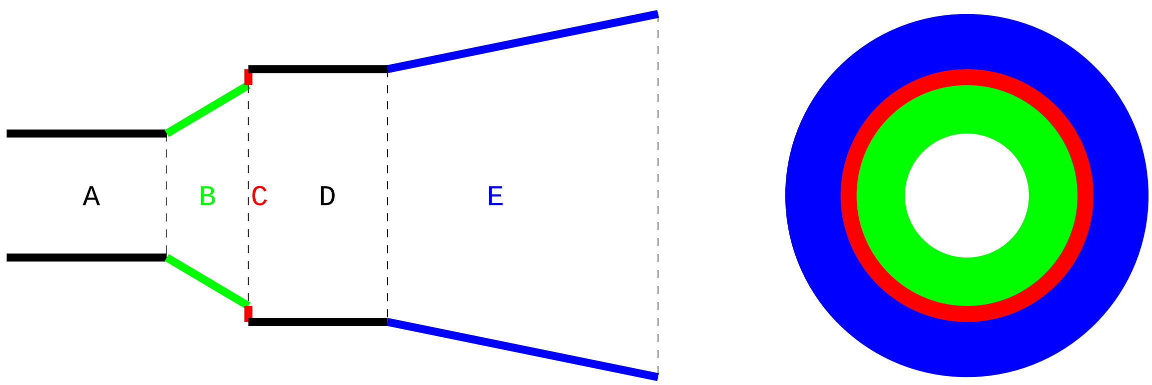

Design of the Potter dual-mode horn is quite complex; Figure 6.5-34 is a sketch. Starting at the left, section **A** is the input circular waveguide, with a diameter such that only the dominant **TE**$_{11}$ mode may propagate. The flared section, **B**, expands this diameter to the desired input diameter for the step transition, **C**, that generates the **TM**$_{11}$ mode. The relative amplitude of the two modes is determined by the two diameters at the step transition, with only the larger output diameter of **D** capable of propagating multiple modes. A constant diameter phasing section, **D**, is used to adjust the phase of the two modes, since they travel at different phase velocities in the waveguide. Finally, the two modes arrive at the throat of the conical horn, **E**, with the desired relative amplitude and phase. The relative phase of the two modes is also shifted by the conical horn, so the length of section **D** must compensate for this phase shift so that the two modes arrive in-phase at the center of the aperture. The fields of the two modes are then out-of-phase at the aperture edges in the E-plane, like Figures 6.5-5, resulting in elimination of the edge currents which create sidelobes in simple conical horns.

The calculations are too involved to include here, and a careful reading of Potter's paper[14] is recommended. The equation for phase shift in the flared conical horn has *eight* terms, with Bessel functions needed for each term; I have not attempted the calculation. The paper does include some graphical solutions which should be easier to use. Construction also appears quite involved, and he recommends that concentricity and circularity in the order of a few *thousandths* of a wavelength are necessary to prevent spurious waveguide modes. Due to this complexity, I had always thought that this horn would not be useful for hams. However, I recently received email from F4BAY describing his 10 GHz feedhorn. He scaled a 12 GHz DSS horn from an "ASTRA" offset dish to 10.37 GHz and measured the radiation pattern. As I prepared an **NEC2** computer model, I realized that this was a Potter dual-mode conical horn. The calculated radiation patterns, in Figure 6.5-35, show excellent efficiency for an ***f*/D** around 0.6, with a phase center very close to the center of the aperture. The measured data from F4BAY, shown in dashed green lines, is close to the calculated data.

6.5.5 VK2ALU dual-mode feedhorn

VK2ALU has discovered a simpler approach to construction; he was considering the Potter feed as an alternative to the diagonal horn in Figure 6.5-33 to reduce the 45° sidelobe levels. Lyle realized that the W2IMU dual-mode horn uses a simpler method, a flared section, of generating the two modes, and the same method could be applied to a conical dual-mode horn as well. For simplicity, he started with the G3PHO version for 10 GHz, Figure 6.5-7, and added a conical horn to realize a larger aperture. Lyle studied Potter's paper and arrived at a horn length and flare angle that produced the same relative phase at the aperture. The horn is quite long, as can be seen in Figure 6.5-36.

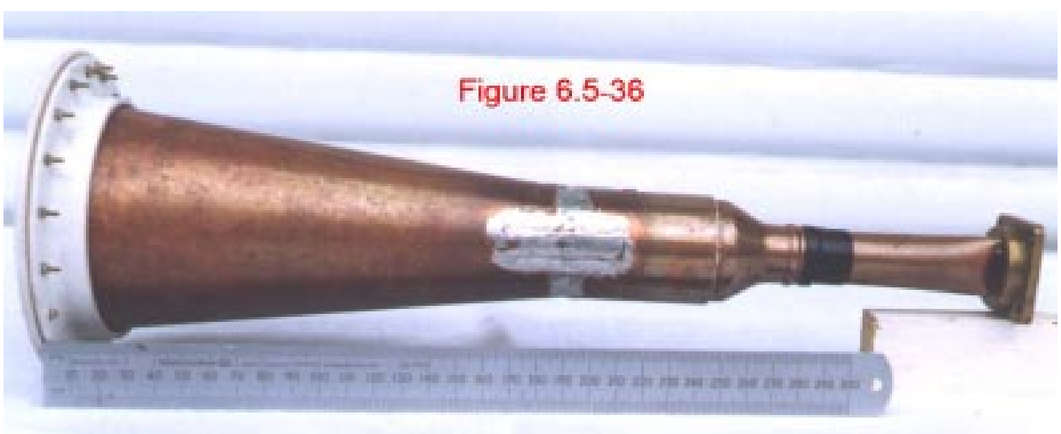
Figure 6.5-36

F4BAY Potter type dual-mode horn for 10.368 GHz, by NEC2

Figure 6.5-35

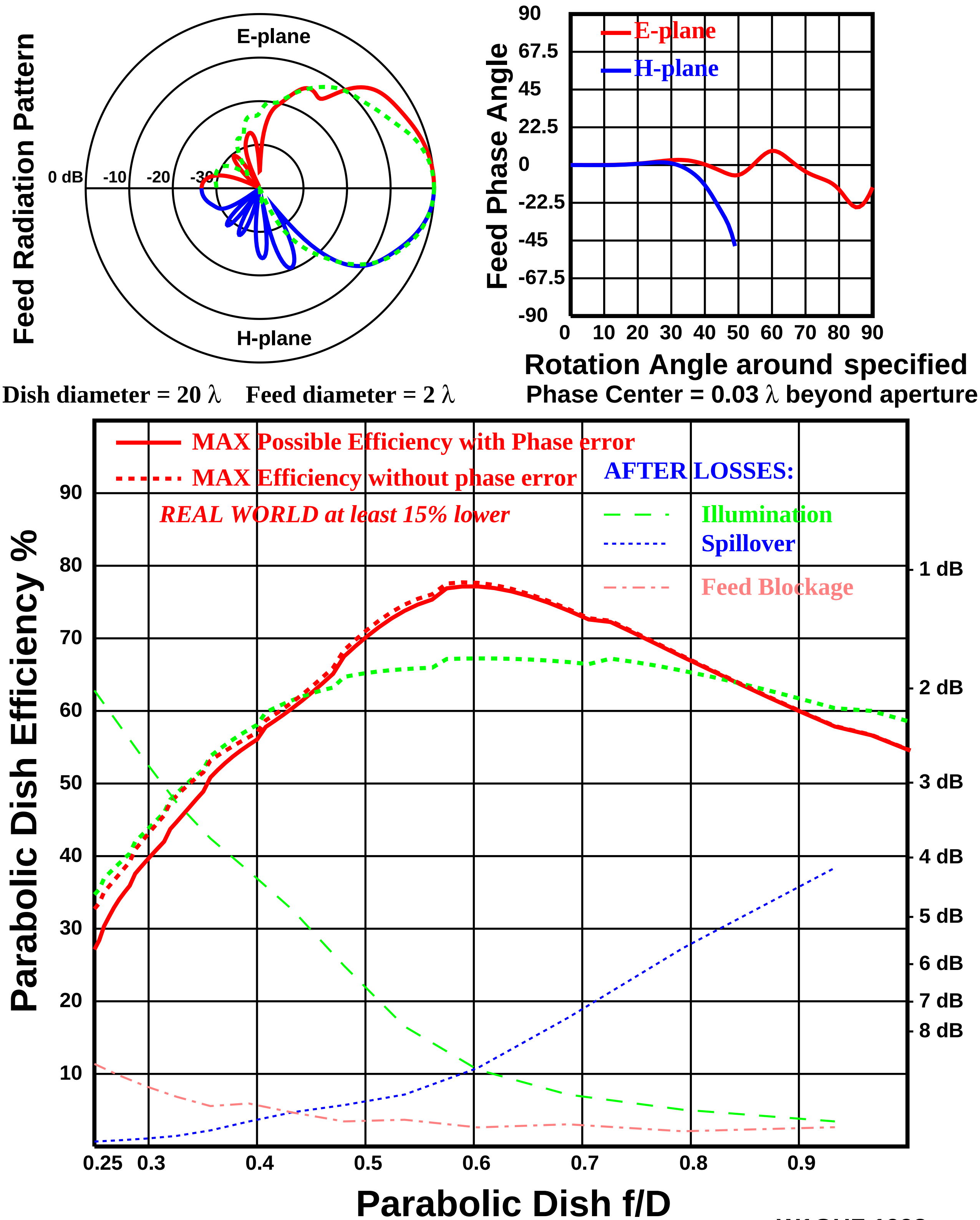

W1GHZ 1998

The length of Lyle's feedhorn was originally too large to calculate using **NEC2** — my PC does not have enough memory — so I calculated approximate radiation patterns using P.O. The results are shown in Figure 6.5-37, with excellent performance for an ***f*/D** around 1.5. Phase center is about 0.4λ inside the aperture. Lyle made careful measurements of the feedhorn radiation pattern; these are also shown in Figure 6.5-37 in dashed green lines. The only difference between the calculated and measured patterns is the first null in the calculated E-plane pattern, which is almost non-existent in the measured pattern. There are at least three possible reasons for this difference:

1. Compromises I made in the calculations.
2. Stray reflections on the antenna range.
3. Small discrepancies in dimensions with fortuitous results.

Later, I was able to use a faster PC with more memory, 128 Megabytes, to run an **NEC2** model for the VK2ALU feedhorn. Even with the larger memory, I was unable to make a fine enough mode, so the calculated radiation patterns have excessive side and back lobes. The **NEC2** patterns are shown in yellow in Figure 6.5-37; the main lobe matches the measured data and P.O. calculations, and shows the same first null in the E-plane pattern.

The VK2ALU dual-mode feed compares favorably with the original 12 GHz corrugated horn of Figure 6.4-22. Lyle is in the process of making sun noise measurements and reports promising initial results.

After I understood Lyle's approach to the dual-mode conical feed, I examined another feedhorn I had lying around. The horn was part of an assembly with two LNBs, usually beige in color; we bought a number of them to convert the LNBs to 10 GHz preamps[15]. The input waveguide to the horn is rather small for 10.368 GHz, just about at cutoff, and there isn't enough metal to bore it out, so I had never tried one. However, the design seemed similar to Lyle's approach, so I made an **NEC2** model for 12 GHz and calculated radiation patterns. Figure 6.5-38 shows the results, with excellent calculated efficiency for an ***f*/D** around 0.7, ideal for an offset dish. The calculated phase center is 0.14λ inside the aperture.

Of course, the next question is, "will it work at 10 GHz?" A simple matter of changing the frequency for the **NEC2** calculations will give us the answer: not very well. The calculated radiation patterns at 10.368 GHz in Figure 6.5-39 have a number of large sidelobes, particularly in the E-plane, and significant phase error, so the calculated efficiency is poor. We can conclude that a dual-mode horn is not broadband; the phase-matching mechanism for the two modes is frequency sensitive.

A photo of this last horn is Figure 6.5-40. The conical horn is much shorter than VK2ALU's horn, since Lyle chose to start with the known phase relationship of the two modes produced by the G3PHO dual-mode horn. The alternative approach, used in the feedhorn in Figure 6.5-40, is to start with a conical horn section of reasonable length and flare angle, then adjust the length of the phasing section, **D** in Figure 6.5-34, to arrive at the desired phase relationship at the aperture. A third approach, the favorite for hams, is to scale a working design to a new frequency; it worked well for F4BAY, and could be applied to this horn as well.

VK2ALU dual-mode feedhorn for 10.368 GHz

Red & Blue = P.O., Green = Measured, Yellow = NEC2

Figure 6.5-37

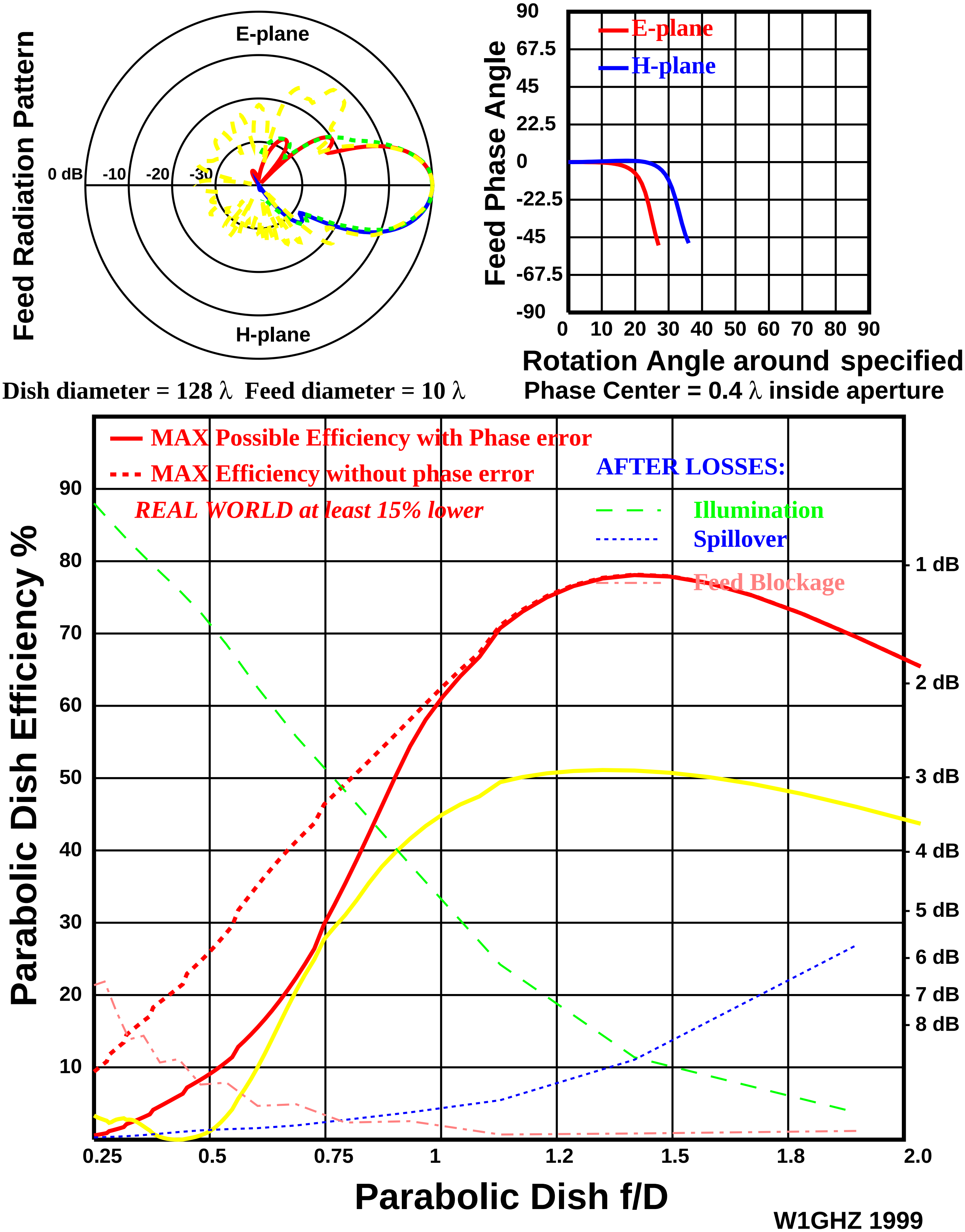

TVRO 12 GHz feedhorn from beige LNB assembly, by NEC2

Figure 6.5-38

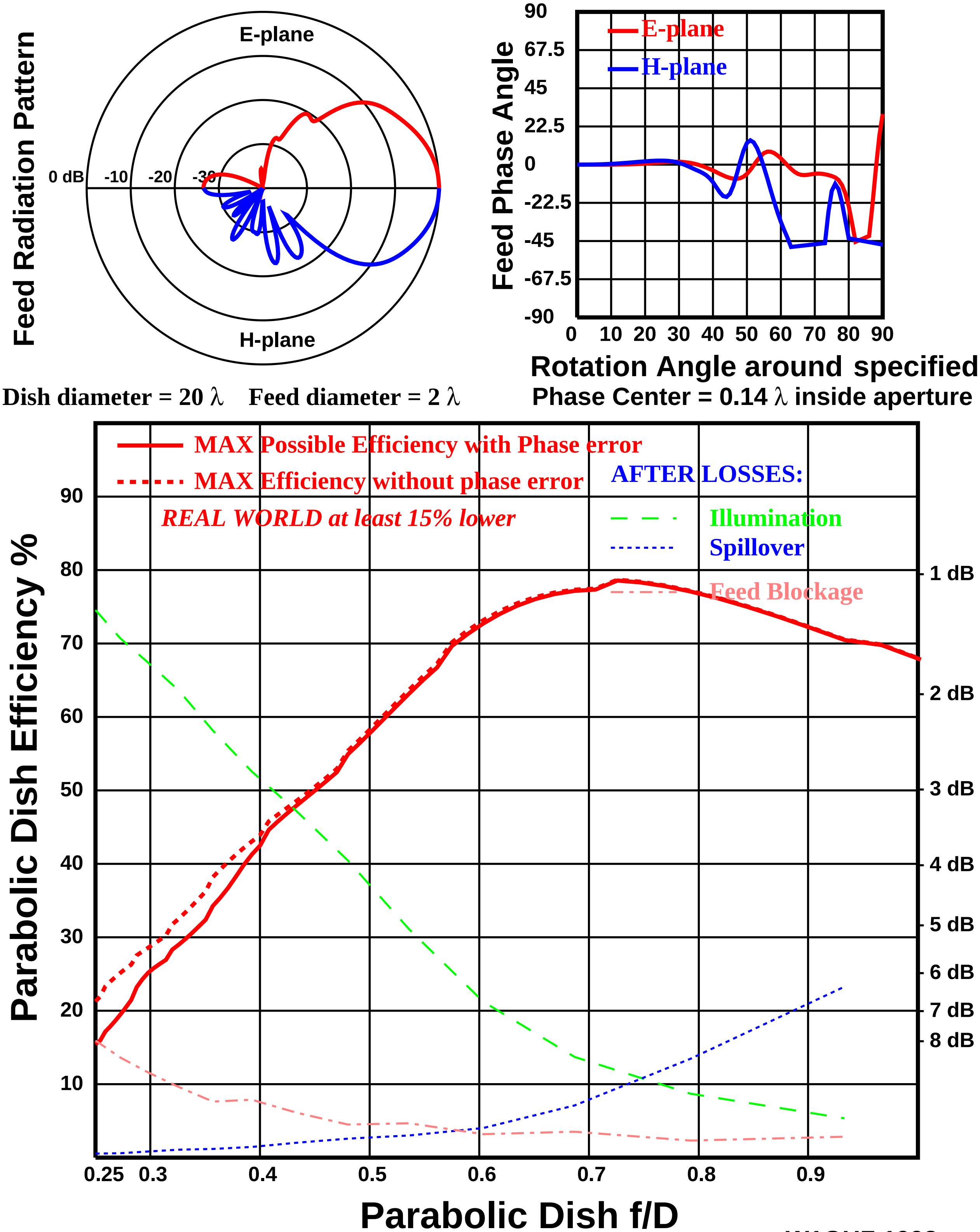

W1GHZ 1998

TVRO feedhorn from beige LNB at 10.368 GHz, by NEC2

Figure 6.5-39

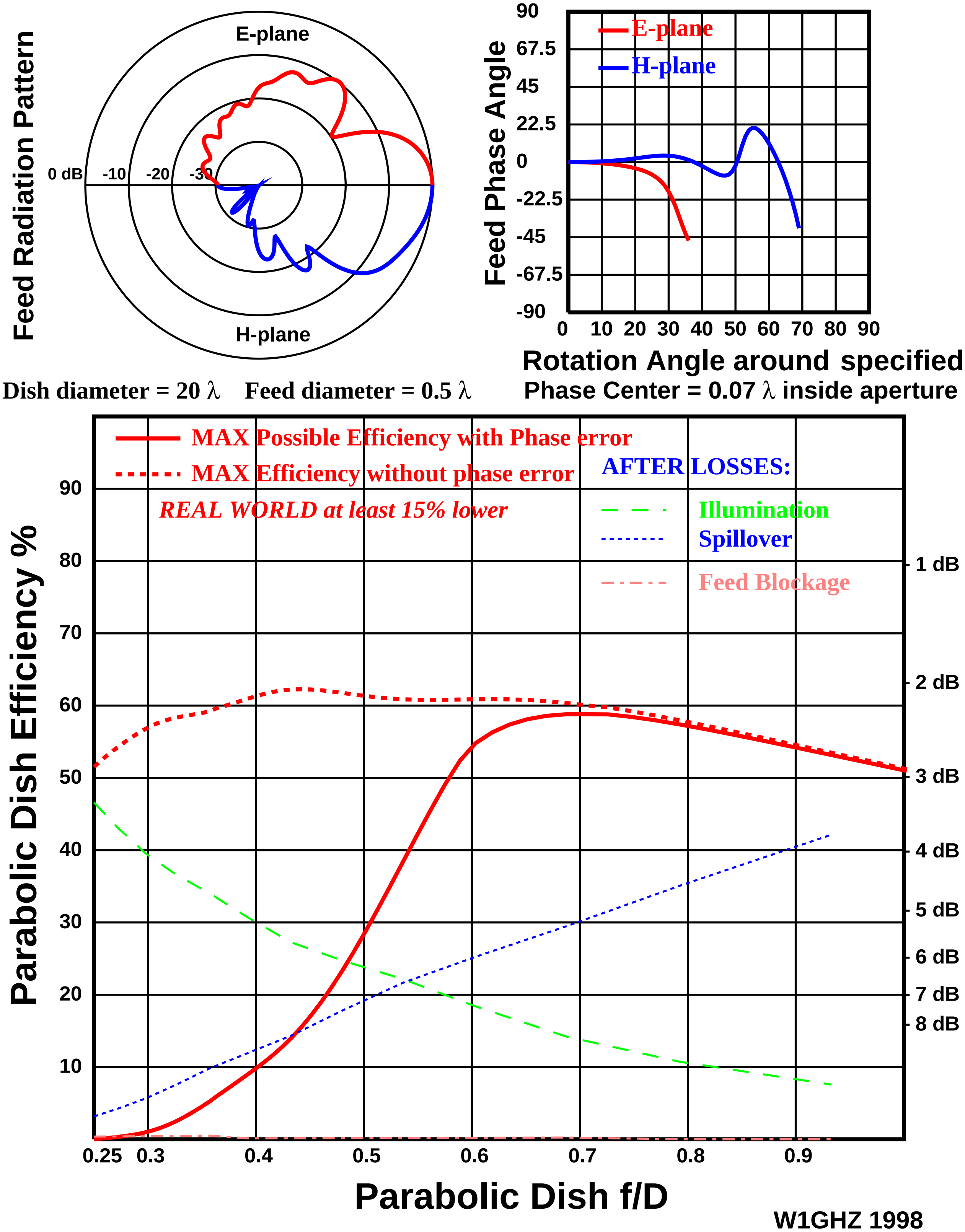

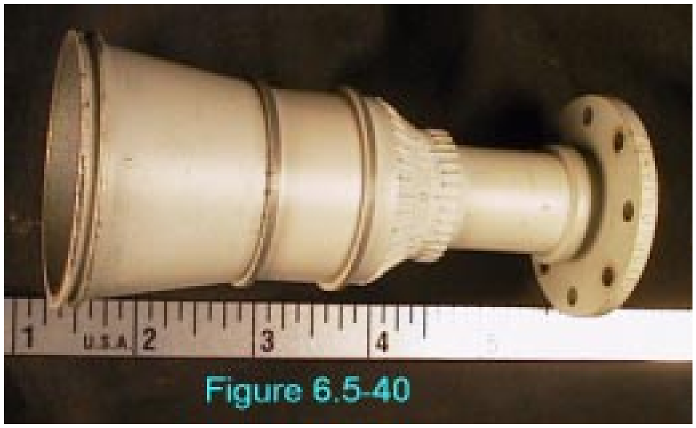

In summary, the Potter dual-mode conical horn offers excellent performance if we are prepared to deal with some complexity. The VK2ALU approach of combining the W2IMU dual-mode design with a conical horn has the potential for maintaining the performance while reducing complexity, and has been used in commercial feeds as well.

6.5.6 Higher-order multi-mode feeds

Several books make reference to tri-mode and higher order feeds, but I have not been able to locate any of the references given, so I don't know whether they are feasible. Ludwig[16] describes performance improvements using three and four mode horns but gives no hint how these might be constructed.

Since we have already discussed a number of feeds capable of providing very good performance, our efforts might be better spent in implementing one of these and using it rather than searching further for the ultimate feed.

6.5 References (continued)

11. A.W. Love, "The Diagonal Horn Antenna," *Microwave Journal*, March 1962, pp. 117-122. (reprinted in A.W. Love, *Electromagnetic Horn Antennas*, IEEE, 1976, pp. 189-194.)

12. R. Miller, N7ART, "A 23cm Diagonal Waveguide Feed," ***DUBUS***, 2/1997, pp. 5-14.

13. D. Turrin, W2IMU, "Parabolic Reflector Antennas and Feeds," *The ARRL UHF/Microwave Experimenter's Manual*, ARRL, 1990, p. 9-29.

14. P.D. Potter, "A New Horn Antenna with Suppressed Sidelobes and Equal Beamwidths," *Microwave Journal*, June 1963, pp. 71-78. (reprinted in A.W. Love, *Electromagnetic Horn Antennas*, IEEE, 1976, pp. 195-202.)

15. P. Wade, N1BWT, and D. Twombly, WB1FKF, "Modification of TVRO LNBs for 10 GHz," ***QEX***, April 1995, pp. 3-5.

16. A.C. Ludwig, "Radiation Pattern Synthesis for Circular Aperture Horn Antennas," *IEEE Transactions on Antennas and Propagation*, July 1966, pp. 434-440. (reprinted in A.W. Love, *Electromagnetic Horn Antennas*, IEEE, 1976, pp. 207-213.)